

Iryna Sushko (Institute of Mathematics of the National Academy of Sciences of Ukraine, Kyiv),

Laura Gardini¹ (Department of Economics, Society and Politics, University of Urbino, Italy),

Kiminori Matsuyama (Department of Economics, Northwestern University, USA)

1D PIECEWISE SMOOTH MAP: EXPLORING A MODEL OF INVESTMENT DYNAMICS UNDER FINANCIAL FRICTIONS WITH THREE TYPES OF INVESTMENT PROJECTS

ОДНОВИМІРНЕ КУСКОВО-ГЛАДКЕ ВІДОБРАЖЕННЯ: ДОСЛІДЖЕННЯ МОДЕЛІ ІНВЕСТИЦІЙНОЇ ДИНАМІКИ В УМОВАХ ФІНАНСОВОГО ТЕРТЯ З ТРЬОМИ ТИПАМИ ІНВЕСТИЦІЙНИХ ПРОЄКТІВ

We consider a 1D continuous piecewise smooth map, which depends on seven parameters. Depending on the values of parameters, it may have up to six branches. This map was proposed by Matsuyama [Theor. Econ., **8**, 623–651 (2013); Section 5]. It describes the macroeconomic dynamics of investment and credit fluctuations in which three types of investment projects compete in the financial market. We introduce a partitioning of the parameter space according to different branch configurations of the map and illustrate this partitioning for a specific parameter setting. Then we present an example of the bifurcation structure in a parameter plane, which includes periodicity regions related to superstable cycles. Several bifurcation curves are obtained analytically, in particular, the border-collision bifurcation curves of fixed points. We show that the intersection point of two curves of this kind is an organizing center from which infinitely many other bifurcation curves are originated.

Розглянуто одновимірне неперервне кусково-гладке відображення, яке залежить від семи параметрів і, в залежності від значень цих параметрів, може мати до шести гілок. Це відображення було запропоновано Мацуямо [Theor. Econ., **8**, 623–651 (2013); Section 5] для опису макроекономічної динаміки інвестиційно-кредитних флюктуацій, в якій три види інвестиційних проектів конкурують на фінансовому ринку. Проведено розбиття простору параметрів відповідно до різних конфігурацій гілок відображення. Це розбиття проілюстровано для конкретного набору параметрів. Крім того, наведено приклад біфуркаційної структури у площині параметрів, що включає області періодичності, пов’язані з надстабільними циклами. Кілька біфуркаційних кривих отримано аналітично, зокрема біфуркаційні криві зіткнення з межею нерухомих точок. Показано, що точка перетину двох таких кривих є організуючим центром, що породжує нескінченно багато інших біфуркаційних кривих.

1. Introduction. *Nonsmooth maps* often appear in applied models when some sharp transition in the state space is modelled by means of piecewise smooth functions (see, e.g., the monographs [6, 7, 33] and references therein). Mathematical tools and methods for studying the dynamics of these maps are currently quite well developed, including those used for smooth systems (see, e.g., [9, 12, 27]) and specific for nonsmooth ones [2, 10]. A characteristic property of piecewise smooth maps is related to the existence of a border point(s) (or switching manifold(s) in higher dimensions) that separates the regions of different definitions of the map. By varying some parameter, a *border-collision bifurcation* (BCB for short) can occur when an invariant set of the map (e.g., an attracting fixed point or cycle) collides with a border point, leading to a qualitative change in the dynamics. Typical examples are transitions which cannot occur in smooth maps when, for instance, a BCB of an attracting fixed point leads to an attracting cycle of any period or directly to a chaotic attractor. Since [25], where the notion of border-collision bifurcation was introduced (see also [13, 26]), these bifurcations and related

¹ Corresponding author, e-mail: laura.gardini@uniurb.it.

problems are quite actively studied from both theoretical and applied points of view ([4, 8, 28], to cite a few). An advantage of one-dimensional (1D for short) *continuous* piecewise smooth maps is a possibility to use *skew tent map*, which is a 1D piecewise linear map with one border point (see, e.g., [15, 16, 18, 24]), as a *border-collision normal form*. We refer to [2], where it is explained in detail how to apply the skew tent map to classify possible outcomes of a BCB in a 1D continuous piecewise smooth map.

There are many examples of nonsmooth maps appearing in economic studies. For instance, switching between various regimes occurs in models of innovation dynamics [11, 17, 19], in financial market models [14, 32], in models of investment dynamics under financial frictions [1, 20, 21], etc. The 1D continuous piecewise smooth map considered in the present paper also comes from a model of investment dynamics under financial frictions by Matsuyama [21].

A special case of this model, in which two different types of investment projects compete against each other in the presence of financial frictions, described in Sections 2–4 of [21], has already been studied in detail in [22, 30, 31], where the corresponding map is defined by three branches: increasing, decreasing and flat. In the cited papers, we distinguish between two cases, depending on whether a flat branch is involved in the asymptotic dynamics or not. In the first case, dominant attractors are *superstable cycles*, and in [30] we introduce a modified U-sequence (see [23]) ordering these cycles using their symbolic sequences. In the second case, the resulting map is unimodal, and its dynamics is characterized by not only standard smooth bifurcations, but also BCBs, leading to specific bifurcation structure in the parameter space, including open regions associated with chaotic attractors (this phenomenon is known as *robust chaos*, see [5]).

In this paper, we deal with the model of Section 5 of [21], which features three different types of investment projects competing against one another, where the corresponding map can have up to six branches. This leads to a greater variety of possible BCBs and thus to more interesting bifurcation structures. In particular, we describe an *organizing center* defined as an intersection point of two BCB curves, from which infinitely many other bifurcation curves issue. Recall that such organizing centers are often observed in discontinuous maps, e.g., in Lorenz maps (several examples can be found in [2], see also [3]).

The paper is organized as follows. In Section 2, we first introduce the map and then some preliminary results follow, which are needed to classify the possible cases related to different branch configurations of the map. The definition of the map in each case is given in Appendix. In Section 3, we discuss the bifurcation structure of the parameter space of the map illustrating it by several numerical examples. Section 4 concludes.

2. Preliminaries. The dynamics of the considered model is defined by a family of 1D continuous piecewise smooth maps f given by

$$f(w) = \begin{cases} f_L(w) = w^\alpha, & \text{if } \rho_1(w) > \max\{\rho_2(w), \rho\}, \\ f_M(w) = \left(\frac{\gamma}{\rho} \frac{1}{\max\{(1-w/m_1)/\lambda, 1\}}\right)^\gamma, & \text{if } \rho_1(w) < \rho, \rho_2(w) < \rho, \\ f_R(w) = \left(\frac{\gamma}{B} \frac{\max\{(1-w/m_2)/\mu, 1\}}{\max\{(1-w/m_1)/\lambda, 1\}}\right)^\gamma, & \text{if } \rho_1(w) < \rho_2(w), \rho_2(w) > \rho, \end{cases} \quad (1)$$

where

$$\rho_1(w) = \frac{\gamma}{w^{1-\alpha}} \frac{1}{\max\{(1-w/m_1)/\lambda, 1\}}, \quad \rho_2(w) = \frac{B}{\max\{(1-w/m_2)/\mu, 1\}},$$

and the parameters satisfy the following conditions:

$$0 < \alpha < 1, \quad \gamma = \frac{\alpha}{1-\alpha}, \quad 0 < \mu < 1, \quad m_1 > 0, \quad m_2 > 0, \quad 0 < \lambda < 1, \quad 0 < \rho < B.$$

Map f reduces to the one studied in [30] (see also [22, 31]) for $m_2 = m$, $\lambda = 1$ and $\rho \leq \mu B$. In the present paper, we fix values of the parameters α , μ , B and $m_2 = m$ in the parameter region E defined as follows:

$$E : \begin{cases} B > \gamma \max \left\{ \frac{1}{\mu} \left(1 - \frac{1}{m} \right), m(1-\mu)^{1-1/\alpha} \right\}, \\ B < \gamma \frac{\alpha}{\mu} (m(1-\alpha))^{1-1/\alpha}, \end{cases}$$

and study the bifurcation structure of the (ρ, λ) -parameter plane. In the cited papers, the dynamics of map f is studied in detail, in particular, it is shown that for parameter values belonging to E , map f can have (possibly coexisting) stable and superstable cycles of any period as well as cyclic chaotic intervals of any period; outside E the dynamics of f is rather trivial. Later we recall how the boundaries of region E are obtained (see Section 3).

As an illustrative example, we consider the following case:

$$\alpha = 0.5 \ (\gamma = 1), \quad m_1 = m_2 = m. \quad (2)$$

The region E in this case is defined as

$$E : \begin{cases} B > \max \left\{ \frac{m-1}{\mu m}, \frac{m}{1-\mu} \right\}, \\ B < \frac{1}{\mu m}. \end{cases} \quad (3)$$

In the numerical examples we fix

$$\alpha = 0.5, \quad m_1 = m_2 = 1.2, \quad B = 2.5, \quad \mu = 0.15. \quad (4)$$

It is easy to check that the parameter values given in (4) belong to the region E .

In Fig. 1(e), we present the partitioning of the (ρ, λ) -parameter plane (for other parameter values fixed as in (4)) into the regions related to different branch configurations of map f . All the other figures in Fig. 1 show related examples of map f . We will use these figures to illustrate our reasoning below.

Let us first specify different cases depending on the max-functions in the definition of f . Considering $\max\{(1-w/m_1)/\lambda, 1\}$ and $\max\{(1-w/m_2)/\mu, 1\}$, we introduce the following notations:

$$w = (1-\lambda)m_1 := w_\lambda,$$

$$w = (1-\mu)m_2 := w_\mu.$$

It holds that

$$w_\lambda \leq w_\mu$$

under the assumption (H1):

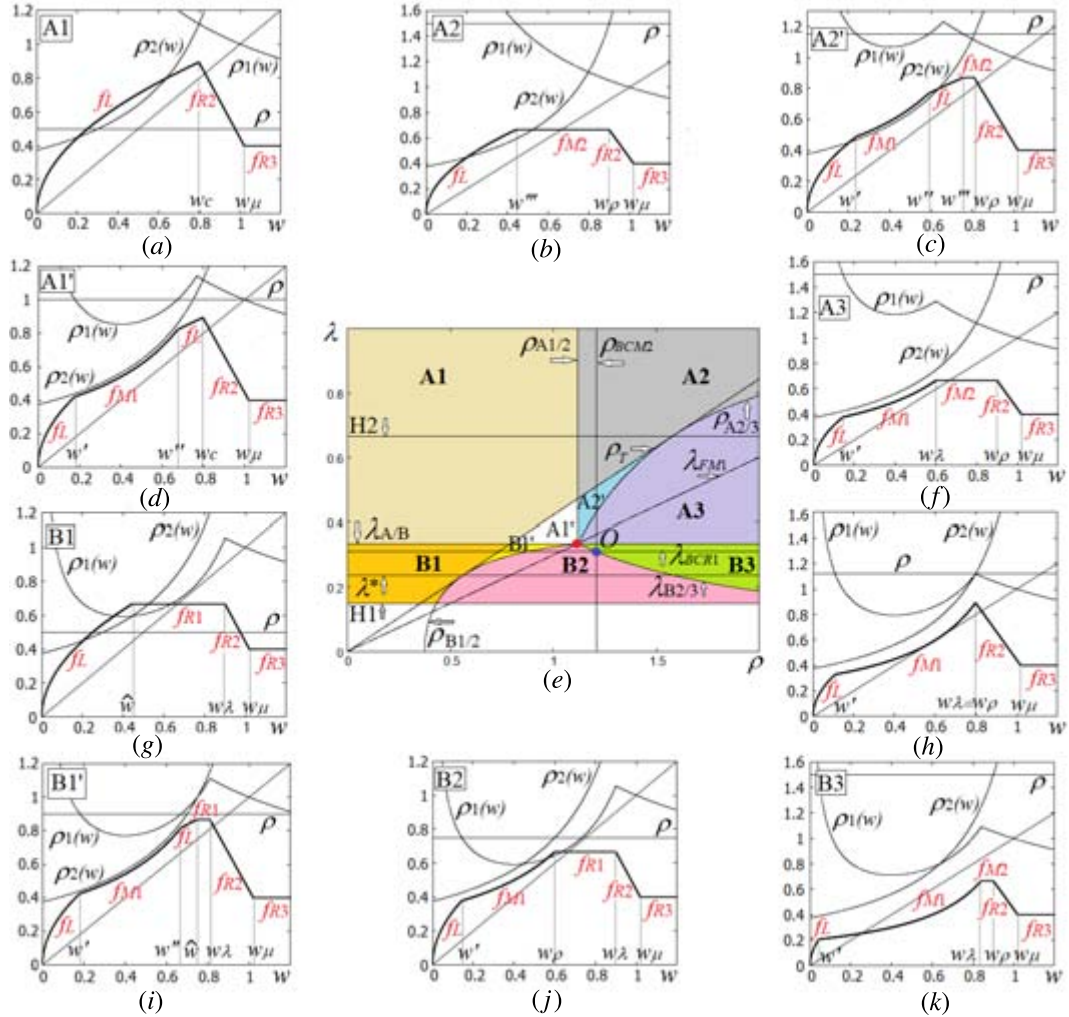


Fig. 1. In (e), a partitioning of the (ρ, λ) -parameter plane into the regions related to different configurations of branches of map f given in (1); other parameter values are as in (4). Example of map f associated with Case A1 (see (10)) for $\rho = 0.5$, $\lambda = 0.8$ (a); A1' (see (11)) for $\rho = 1$, $\lambda = 0.36$ (d); A2 (see (12) for $\rho = 1.5$, $\lambda = 0.8$ (b); A2' (see (13)) for $\rho = 1.15$, $\lambda = 0.45$ (c); A3 (see (15) for $\rho = 1.5$, $\lambda = 0.5$ (f); B1 (see (16) for $\rho = 0.5$, $\lambda = 0.25$ (g); B1' (see (17)) for $\rho = 0.9$, $\lambda = 0.325$ (i); B2 (see (18) for $\rho = 0.75$, $\lambda = 0.25$ (j); and B3 (see (19) for $\rho = 1.5$, $\lambda = 0.3$ (k); in (h), map f for $\rho = \rho_{A1/2}$, $\lambda = \lambda_{A/B}$ (this parameter point is marked by red circle in (e)).

$$\lambda \geq 1 - (1 - \mu) \frac{m_2}{m_1}.$$

In the following considerations we assume that (H1) is satisfied. For the case (2), the equality in (H1) corresponds to

$$H1 : \quad \lambda = \mu$$

(see Fig. 1(e), where $\mu = 0.15$).

According to the introduced notations, the functions $f_M(w)$ and $f_R(w)$ can be defined as

$$f_M(w) = \begin{cases} f_{M1}(w) = \left(\frac{\gamma\lambda}{\rho} \frac{1}{(1-w/m_1)} \right)^\gamma, & \text{if } w \leq w_\lambda, \\ f_{M2}(w) = \left(\frac{\gamma}{\rho} \right)^\gamma, & \text{if } w \geq w_\lambda, \end{cases}$$

$$f_R(w) = \begin{cases} f_{R1}(w) = \left(\frac{\gamma\lambda}{\mu B} \frac{(1-w/m_2)}{(1-w/m_1)} \right)^\gamma, & \text{if } w \leq w_\lambda, \\ f_{R2}(w) = \left(\frac{\gamma}{\mu B} (1-w/m_2) \right)^\gamma, & \text{if } w_\lambda \leq w \leq w_\mu, \\ f_{R3}(w) = \left(\frac{\gamma}{B} \right)^\gamma, & \text{if } w \geq w_\mu. \end{cases}$$

In the special case (2), the branch $f_{R1}(w)$ (which in general is an increasing or decreasing function) becomes constant: $f_{R1}(w) = \frac{\lambda}{\mu B}$.

The functions $\rho_1(w)$ and $\rho_2(w)$ can be defined as

$$\rho_1(w) = \begin{cases} \rho_{1,1}(w) = \frac{\lambda\gamma}{w^{1-\alpha}(1-w/m_1)}, & \text{if } w \leq w_\lambda, \\ \rho_{1,2}(w) = \frac{\gamma}{w^{1-\alpha}}, & \text{if } w \geq w_\lambda, \end{cases}$$

$$\rho_2(w) = \begin{cases} \rho_{2,1}(w) = \frac{B\mu}{(1-w/m_2)}, & \text{if } w \leq w_\mu, \\ \rho_{2,2}(w) = B, & \text{if } w \geq w_\mu. \end{cases}$$

In Fig. 1, besides map f various examples of these functions are also shown.

Consider now the possible solutions of the equation $\rho_1(w) = \rho$. The branch $\rho_{1,2}(w)$ of $\rho_1(w)$ is a decreasing function, while the branch $\rho_{1,1}(w)$ is a unimodal function with an extremum (minimum) at

$$w = \frac{m_1(1-\alpha)}{(2-\alpha)} := w^*.$$

It holds that $w^* > w_\lambda$ for $\lambda > \frac{1}{2-\alpha}$, that is, in this case both branches of $\rho_1(w)$ are decreasing. Thus, a sufficient condition to have a unique solution of the equation $\rho_1(w) = \rho$ is (H2):

$$\lambda \geq \frac{1}{2-\alpha}.$$

For (2), the equality in (H2) corresponds to

$$H2 : \quad \lambda = \frac{2}{3}$$

(see Fig. 1(e)).

If the assumption (H2) does not hold, that is, if $\lambda < \frac{1}{2-\alpha}$ (so that $w^* < w_\lambda$), then

- for $\rho_{1,1}(w^*) < \rho < \rho_{1,1}(w_\lambda) = \rho_{1,2}(w_\lambda)$, the equation $\rho_1(w) = \rho$ has three solutions denoted $w' < w'' < w'''$, where $w = w'$, $w = w''$ are two solutions of $\rho_{1,1}(w) = \rho$, and $w = w''' = \left(\frac{\gamma}{\rho} \right)^{\frac{1}{1-\alpha}}$

is a solution of $\rho_{1,2}(w) = \rho$ (see an example in Fig. 1(c)); this case occurs for

$$\rho_T < \rho < \rho_{A2/3},$$

where

$$\rho = \rho_{1,1}(w^*) = \frac{\gamma\lambda(2-\alpha)^{2-\alpha}}{((1-\alpha)m_1)^{1-\alpha}} := \rho_T \quad (5)$$

and

$$\rho = \rho_{1,1}(w_\lambda) = \rho_{1,2}(w_\lambda) = \frac{\gamma}{((1-\lambda)m_1)^{1-\alpha}} := \rho_{A2/3} \quad (6)$$

(the index $A2/3$ is clarified in Appendix, see (14));

- for $\rho > \rho_{A2/3}$, the unique solution of $\rho_1(w) = \rho$ is $w = w'$ (see an example in Fig. 1(f));
- for $\rho < \rho_T$, the unique solution of $\rho_1(w) = \rho$ is $w = w'''$.

For (2), the equalities (5) and (6) become

$$\rho = \frac{3\lambda}{2} \sqrt{\frac{3}{m}} = \rho_T \quad \text{and} \quad \rho = \frac{1}{\sqrt{(1-\lambda)m}} = \rho_{A2/3}$$

(see the curves ρ_T and $\rho_{A2/3}$ in Fig. 1(e), where $m = 1.2$).

The solution of $\rho_2(w) = \rho$ is

$$w = \left(1 - \frac{\mu B}{\rho}\right) m_2 := w_\rho.$$

For $\rho < B$, as required, it is unique, and it holds that

$$w_\rho < w_\mu.$$

The definition regions of the various branches of f depend also on an intersection point of $\rho_1(w)$ and $\rho_2(w)$. Let it be denoted

- w_c when $w_c \geq w_\lambda$, i.e., when it is related to the branch $\rho_{1,2}(w)$ of $\rho_1(w)$, i.e., $\rho_{1,2}(w_c) = \rho_2(w_c)$, or

$$\frac{\gamma}{w_c^{1-\alpha}} = \frac{B\mu}{(1 - w_c/m_2)}$$

(see an example in Fig. 1(d));

- \hat{w} when $\hat{w} \leq w_\lambda$, i.e., when it is related to the branch $\rho_{1,1}(w)$ of $\rho_1(w)$, i.e., $\rho_{1,1}(\hat{w}) = \rho_2(\hat{w})$, or

$$\frac{\lambda\gamma}{\hat{w}^{1-\alpha}(1 - \hat{w}/m_1)} = \frac{B\mu}{(1 - \hat{w}/m_2)} \quad (7)$$

(see an example in Fig. 1(g)); note that if $\lambda < \frac{1}{2-\alpha}$ and $\rho_T < \rho < \rho_{A2/3}$ (when there are two solutions of the equation $\rho_{1,1}(w) = \rho$), then $\hat{w} < w^*$ is a sufficient condition for the inequality $\rho_1(w) > \max\{\rho_2(w), \rho\}$ (definition condition for the branch f_L , see (1)) to be satisfied in just one interval; it holds that $\hat{w} = w^*$, that is, $\rho_{1,1}(w^*) = \rho_2(w^*)$ for

$$\lambda = \left(\frac{m_1(1-\alpha)}{(2-\alpha)} \right)^{1-\alpha} \frac{B\mu m_2}{\gamma((2-\alpha)m_2 - m_1(1-\alpha))} := \lambda^*, \quad (8)$$

and $\hat{w} < w^*$ for $\lambda < \lambda^*$; for (2), we have

$$\lambda = \sqrt{\frac{m}{3}} B\mu = \lambda^*$$

(see Fig. 1(e)).

Let us summarize now the preliminary observations presented above and distinguish between different branch configurations of map f . It is convenient to divide them into two cases, when $w_\lambda < w_c$ (denoted as **Case A**) and $w_\lambda > w_c$ (**Case B**), with further division into subcases, **A1**, **A1'**, **A2**, **A2'**, **A3** and **B1**, **B1'**, **B2**, **B3**, as explained in Appendix. In Fig. 1(e), we present the partitioning of the (ρ, λ) -parameter plane according to these subcases, and in the figures around Fig. 1(e), related examples of map f are shown (see Appendix for the definition of map f in each case). Since $w_\lambda < w_c$ for $\lambda > 1 - \frac{w_c}{m_1}$, the transition from Case A to Case B occurs at

$$\lambda = 1 - \frac{w_c}{m_1} := \lambda_{A/B}. \quad (9)$$

For (2), this transition occurs at

$$\lambda = 1 - \frac{w_c}{m} = \lambda_{A/B}, \quad \text{where} \quad w_c = 0.25(-m\mu B + \sqrt{(m\mu B)^2 + 4m})^2.$$

As one can see in Fig. 1(e), above the line $H2$ only the cases **A1**, **A2** and **A3** can occur; in the strip between the lines $H1$ and λ^* only the cases **B1**, **B2** and **B3** can occur; and in the strip between the lines λ^* and $H2$ all the cases can be realized. In particular, for the parameter values belonging to the region bounded by the curves ρ_T , $\rho_{A2/3}$ and $\rho_{B1/2}$, there are regions associated with cases **A1'**, **A2'** and **B1'**, whose distinguishing feature is the presence in f of two definition intervals of the branch f_L .

In Fig. 1(h), we show map f at a special parameter point $(\rho, \lambda) = (\rho_{A1/2}, \lambda_{A/B})$ indicated by the red circle in Fig. 1(e), from which the boundaries of several partitions issue. One could expect that this point is a kind of organizing center from which infinitely many bifurcation curves issue. However, the true organizing center in the (ρ, λ) -parameter plane is an intersection point O (indicated by the blue circle in Fig. 1(e)) of two BCB curves, $\rho = \rho_{BCM2}$ and $\lambda = \lambda_{BCR1}$, as we discuss in the next section.

3. Bifurcation structures in the parameter space. Before we proceed with a description of the bifurcation structure of the (ρ, λ) -parameter plane, let us recall in short what is known about the dynamics of map f in case **A1** (see (10)). These results are summarized in Fig. 2 (for details, see [22, 30, 31]). Namely, in Fig. 2(a) we show the bifurcation structure of the (μ, B) -parameter plane for $\alpha = 0.5$, $m = 1.2$ (as in (4)). Here the region E (see (3)) is bounded by the bifurcation curves of the fixed points w_L^* , w_{R2}^* and w_{R3}^* associated with the branches f_L , f_{R2} and f_{R3} , respectively:

- the curve defined by $B = \frac{1}{\mu} \left(1 - \frac{1}{m} \right)$ (denoted BC_L) is related to a BCB at which $w_L^* = 1 = w_{R2}^*$;
- the curve $B = \frac{1}{\mu m}$ (denoted FB_{R2}) is related to a degenerate flip bifurcation of w_{R2}^* (see [29], where degenerate bifurcations are described);

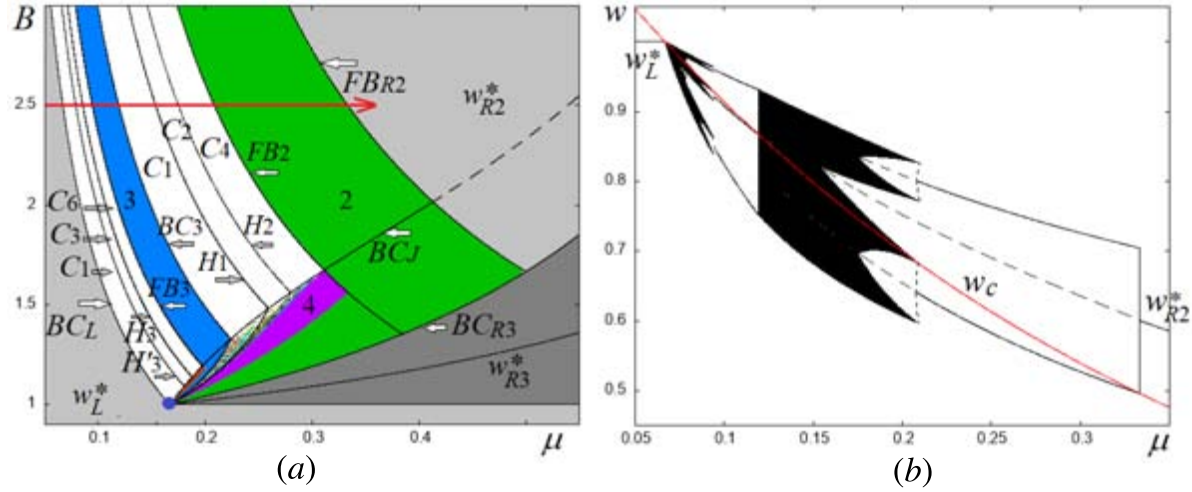


Fig. 2. (a) Bifurcation structure of the (μ, B) -parameter plane of map f in case A1 (see (10)). The region E (see (3)) is bounded by the curves BC_L , BC_{R3} and FB_{R2} ; other parameters are fixed as in (4); white regions are related to n -cyclic chaotic intervals C_n and colored regions to attracting cycles (some regions are marked by numbers which are periods of the related cycles); (b) 1D bifurcation diagram corresponding to the cross-section at $B = 2.5$ of the 2D diagram shown in (a) (the related parameter path is indicated in (a) by the red arrow).

- the curve $B = \frac{1}{m(1-\mu)}$ (denoted BC_{R3}) corresponds to a BCB at which $w_{R3}^* = w_\mu = w_{R2}^*$.

Other curves shown in Fig. 2(a) are FB_2 (subcritical flip bifurcation of 2-cycle denoted γ_2), H_2 (homoclinic bifurcation of γ_2), H_1 (homoclinic bifurcation of w_{R2}^*), BC_3 (fold BCB leading to a pair of 3-cycles, attracting γ_3 and repelling γ'_3), FB_3 (subcritical flip bifurcation of γ_3), H_3 (homoclinic bifurcation of γ_3), H'_3 (homoclinic bifurcation of γ'_3), BC_J (contact of the absorbing interval $J = [f^2(w_c), f(w_c)]$ with the flat branch f_{R3} , occurring when $f(w_c) = w_\mu$; below BC_J the flat branch f_{R3} is involved into asymptotic dynamics, so that the dominant dynamics of map f are superstable cycles). White regions in Fig. 2(a) are related to n -cyclic chaotic intervals C_n . For parameter values outside E map f has globally attracting fixed points.

To illustrate the bifurcations mentioned above we show in Fig. 2(b) a 1D bifurcation diagram μ versus w , where $0.05 < \mu < 0.35$, $B = 2.5$ (the corresponding parameter path is marked in Fig. 2(a) by red arrow). It can be seen, in particular, that for $\mu = 0.15$ (as in (4)), map f has a one-piece chaotic attractor, $C_1 = [f^2(w_c), f(w_c)]$. This means that for parameter values belonging to the region marked A1 in Fig. 1(e), an attractor of map f is the chaotic interval C_1 .

Now let us turn to the bifurcation structure of the (ρ, λ) -parameter plane. We first obtain conditions of the simplest bifurcations related to the fixed points of map f :

- A BCB of the fixed point w_{R1}^* of $f_{R1}(w)$, which is a solution of

$$\left(\frac{\gamma \lambda}{\mu B} \frac{(1 - w_{R1}^*/m_2)}{(1 - w_{R1}^*/m_1)} \right)^\gamma = w_{R1}^*,$$

occurs when w_{R1}^* collides with the border point w_λ , that is, when $w_{R1}^* = (1 - \lambda)m_1$. For (2), we have $w_{R1}^* = \frac{\lambda}{\mu B}$, so that the BCB curve is given by

$$\lambda = \frac{m\mu B}{1 + m\mu B} =: \lambda_{BCR1}.$$

- A BCB of the fixed point w_{M2}^* of $f_{M2}(w)$ occurs when $f_{M2}(w) = w_\rho$, that is, when

$$\left(\frac{\gamma}{\rho}\right)^\gamma = \left(1 - \frac{\mu B}{\rho}\right)m_2,$$

and for (2) it occurs when

$$\rho = \frac{1}{m} + \mu B := \rho_{BCM2}.$$

- A fixed point w_{M1}^* of $f_{M1}(w)$ satisfies

$$\left(\frac{\gamma\lambda}{\rho} \frac{1}{(1 - w_{M1}^*/m_1)}\right)^\gamma = w_{M1}^*.$$

In case (2), we have

$$w_{M1\pm}^* = \frac{1}{2}(m \pm \sqrt{m^2 - 4m\lambda/\rho}),$$

and a fold bifurcation occurs when the two points are merging, i.e., at

$$\lambda = \frac{m\rho}{4} =: \lambda_{FM1}.$$

The bifurcation curves λ_{BCR1} , ρ_{BCM2} and λ_{FM1} , obtained above are shown in Fig. 1(e), as well as in Fig. 3(a).

In Fig. 3(a) we present bifurcation structure of the (ρ, λ) -parameter plane (an enlarged window of Fig. 1(e)), obtained numerically, where periodicity regions related to attracting cycles of different periods are shown by different colors. Since map f in the considered parameter region may have up to six branches, it is a challenging task to give a complete description of this bifurcation structure. However, the presence of flat branches in the definition of f simplifies such a description, given that the dominant dynamics in maps with flat branches are associated with superstable cycles and their BCBs. As we already mentioned, it occurs in region E below the curve BC_J in Fig. 2(a), related to map f in case A1, when the flat branch f_{R3} is involved into asymptotic dynamics. We refer to [30] for details, where in particular so-called modified U-sequence is introduced, which orders the superstable cycles using their symbolic sequences. Similar structures are observed also in Fig. 3(a), however, here more border points are involved into BCBs.

To clarify possible bifurcation sequences, we present in Fig. 3(b) a 1D bifurcation diagram for fixed $\lambda = 0.36$ and $1.115 < \rho < 1.22$ (the related parameter path is indicated in Fig. 3(a) by red arrow). It is convenient to comment this diagram for decreasing values of ρ . Our starting point is in the region related to Case A3 (see (15)), below the curve λ_{FM1} , when a superstable fixed point $w_{M2}^* = f_{M2} = 1/\rho$ coexists with an attracting fixed point w_{M1-}^* (this point is outside the window shown in Fig. 3(b)). See an example of map f and its attractors in this case in Fig. 4(a). For decreasing ρ , a flip BCB² occurs at which w_{M2}^* collides with border point w_ρ , leading to a superstable 2-cycle $\{1/\rho, f_{R2}(1/\rho)\}$ (see an example in Fig. 4(b)). Note that using the skew tent map as a border-collision normal form, it is easy to show (see, e.g., [30]) that a superstable fixed

²It is worth to emphasize that a flip BCB or a fold BCB of a fixed point (or cycle) is related not to an eigenvalue -1 or 1 , but to a collision of the fixed point (or a periodic point) with a border point.

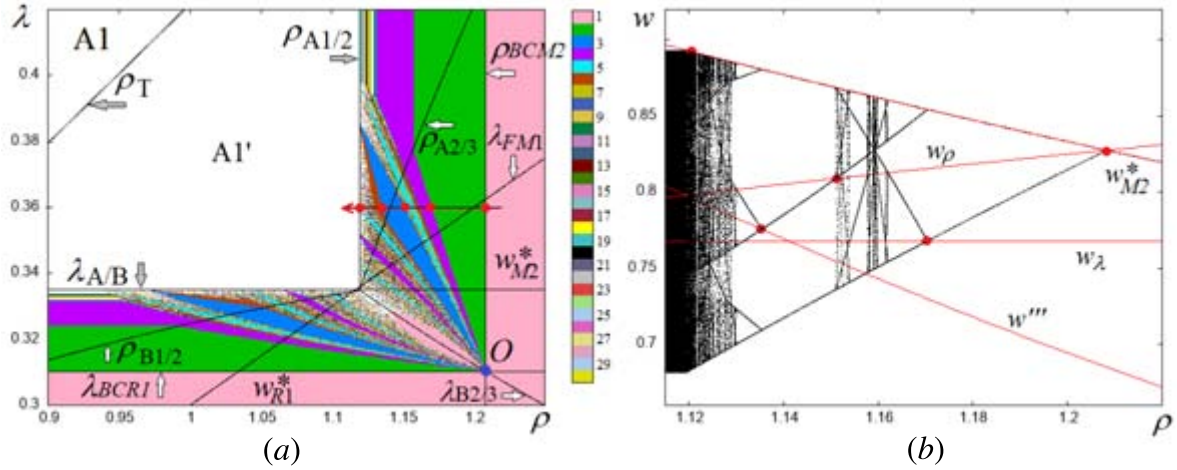


Fig. 3. (a) 2D bifurcation diagram in the (ρ, λ) -parameter plane for other parameter values fixed as in (4); (b) 1D bifurcation diagram ρ versus w for $1.115 < \rho < 1.22$, $\lambda = 0.36$.

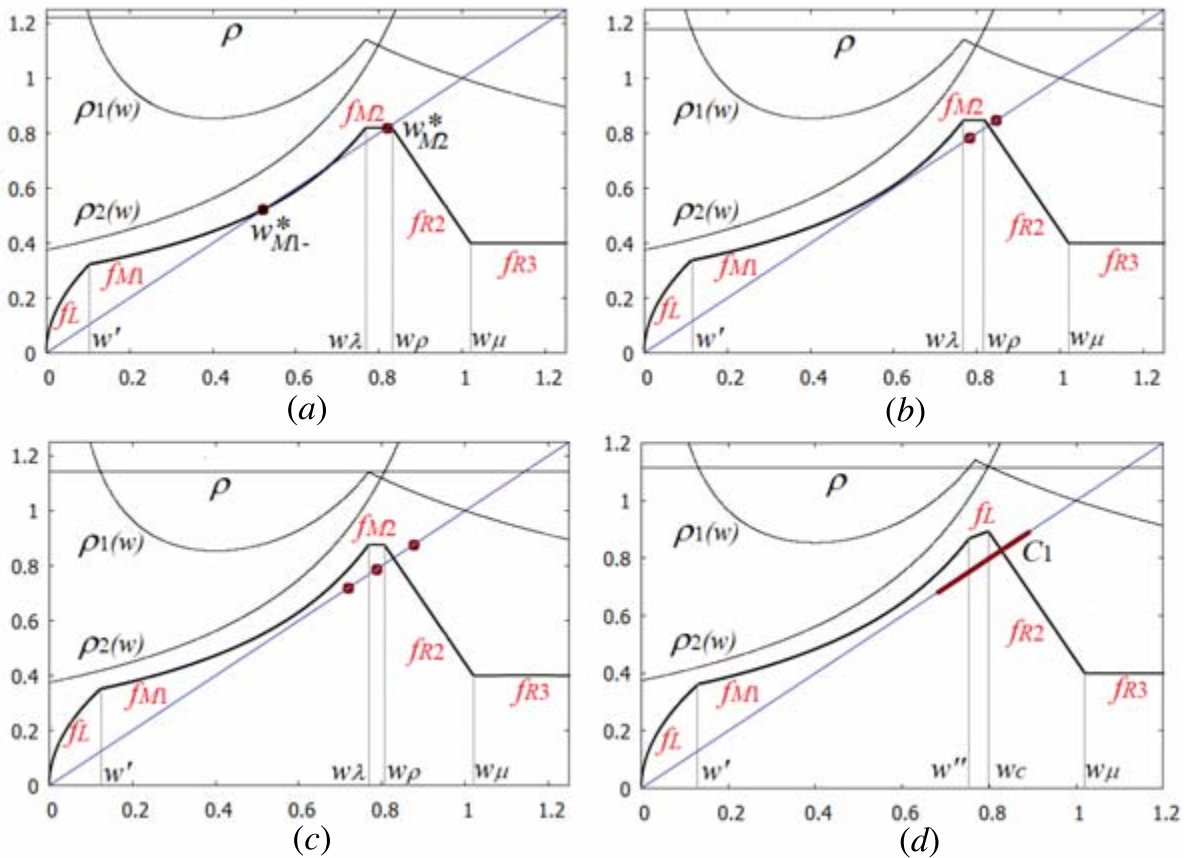


Fig. 4. Examples of map f and its attractors for $\lambda = 0.36$ and (a) $\rho = 1.22$; (b) $\rho = 1.18$; (c) $\rho = 1.141$; (d) $\rho = 1.115$. Other parameters are as in (4).

point (or cycle) can undergo either a flip BCB, or a fold BCB, or a persistence border collision (leading to an attracting fixed point or cycle). Next BCB occurs when this 2-cycle collides with

border point w_λ leading to a 4-cycle which also includes the point $w = 1/\rho$ (in fact, all the cycles of map f in Fig. 3(b) for $\rho > \rho_{A1/2}$ consist of the point $w = 1/\rho$ and its images). A cascade of flip BCB follows, with alternating border points w_ρ and w_λ , which accumulates, similar to the 'smooth' period-doubling cascade, to a specific parameter point, an analog of the Feigenbaum accumulation point. One more bifurcation, which is clearly seen in Fig. 3(b), is a fold BCB with border point w_ρ leading to a superstable 3-cycle (see Fig. 4(c)). For further decreasing ρ , the parameter point enters the region related to Case A2' (see (13)). Next BCB occurs when the 3-cycle collides with border point $w = w''$, leading to a superstable 6-cycle, followed by a flip BCB cascade. One more bifurcation indicated in Fig. 3(b) occurs at $\rho = \rho_{A1/2}$, at which the chaotic interval $C_1 = [f_{R2}^2(w_c), f_{R2}(w_c)]$ (an example is shown in Fig. 4(d)) for increasing ρ disappears due to the appearance of the flat branch f_{M2} .

Consider now an intersection point of two BCB curves, $\rho = \rho_{BCM2}$ and $\lambda = \lambda_{BCR1}$ (see point O in Fig. 3(a)). It is an organizing center from which infinitely many other bifurcation curves issue which are BCB boundaries of the periodicity regions related to superstable cycles of map f . To see this, consider a neighborhood of O overlapping with region B3, where map f has flat branch f_{M2} , see (19) (it has also the flat branch f_{R3} , but for the considered parameter values this branch is not involved into asymptotic dynamics). Any superstable cycle of map f includes point $w = f_{M2} = 1/\rho$ and its images, thus two superstable cycles cannot coexist, so that their periodicity regions are not overlapping. Approaching point O , two BCB boundaries of a periodicity region (one related to the collision of a periodic point with $w = w_\rho$ and the other one with $w = w_\lambda$) tend to each other merging at point O at which $w_\rho = w_\lambda = w_{R1}^* = w_{M2}^*$. Similar bifurcation structure is observed in a neighborhood of O overlapping with region B2, where map f has flat branch f_{R1} , see (18). All the periodicity regions (with blocks of joined regions related to the same flip BCB cascade) can be ordered according to a modified U-sequence in a similar way as it is done in [30] for the periodicity regions of the superstable cycles in the (μ, B) -parameter plane in region E below the curve BC_J (see Fig. 2(a)). Indeed, in Fig. 2(a), an intersection point (indicated by blue circle) of the BCB curves BC_L and BC_{R3} , which is $(\mu, B) = (1 - 1/m, 1)$, is also an organizing center of a similar kind as point O . Note that organizing centers are often observed in the parameter space of discontinuous maps (see, e.g., [2] where several kinds of organizing centers in Lorenz maps are described).

4. Conclusion. The present paper can be considered as a starting point for a detailed investigation of the dynamics of the Matsuyama model in a more generic case. We described partitioning of the parameter space of the corresponding map into the regions related to different branch configurations of this map. This partitioning was presented for a specific parameter setting which allowed us to get several bifurcation curves analytically. The obtained results were illustrated by 1D and 2D bifurcation diagrams. Since the considered map depends on seven parameters, while in the present work five of them were fixed, more work is needed to get a complete description of possible bifurcation sequences. From the dynamical view point, we expect to observe new interesting bifurcation structures associated with the interplay of several (up to five) border points. The detailed investigation of possible organizing centers related to the collisions with different border points is also left for a future work.

Appendix.

Case A: $w_\lambda < w_c$. Let $w_\lambda < w_c$, i.e., $\lambda > \lambda_{A/B}$ where $\lambda_{A/B}$ is given in (9) (see the region above the line $\lambda_{A/B}$ in Fig. 1(e)). We need to distinguish between the following subcases depending on the value of ρ .

Suppose first that $\rho < \rho_1(w_c) = \rho_2(w_c) =: \rho_{A1/2}$ and $\rho < \rho_T$ (see (5)). In this case, denoted **A1**, map f is identical to the one studied in [30] (see also [22, 31]) with $m_2 = m$:

$$(A1) \quad f(w) = \begin{cases} f_L(w) = w^\alpha, & \text{if } w < w_c, \\ f_{R2}(w) = \left(\frac{\gamma}{\mu B}(1 - w/m_2)\right)^\gamma, & \text{if } w_c < w < w_\mu, \\ f_{R3}(w) = \left(\frac{\gamma}{B}\right)^\gamma, & \text{if } w > w_\mu. \end{cases} \quad (10)$$

Here the branch $f_L(w)$ is increasing and concave, $f_{R2}(w)$ is decreasing (linear if $\alpha = 1/2$, convex if $\alpha < 1/2$ and concave if $\alpha > 1/2$), and $f_{R3}(w)$ is flat. Example of map f in case A1 is shown in Fig. 1(a).

If $\rho < \rho_{A1/2}$ and $\rho > \rho_T$ (Case **A1'**), branch $f_{M1}(w)$ (increasing and convex) appears in the definition of f (and branch f_L is defined in two intervals):

$$(A1') \quad f(w) = \begin{cases} f_L(w) = w^\alpha, & \text{if } w < w', \\ f_{M1}(w) = \left(\frac{\gamma\lambda}{\rho}\frac{1}{(1 - w/m_1)}\right)^\gamma, & \text{if } w' < w < w'', \\ f_L(w) = w^\alpha, & \text{if } w'' < w < w_c, \\ f_{R2}(w) = \left(\frac{\gamma}{\mu B}(1 - w/m_2)\right)^\gamma, & \text{if } w_c < w < w_\mu, \\ f_{R3}(w) = \left(\frac{\gamma}{B}\right)^\gamma, & \text{if } w > w_\mu \end{cases} \quad (11)$$

(see an example in Fig. 1(d)).

The transition **A1/A2** (as well as **A1'/A2'**) occurs when $\rho = \rho_1(w_c) = \rho_2(w_c) = \rho_{A1/2}$. For the special case (2), we have $\rho_1(w_c) = \rho_2(w_c) = \frac{1}{\sqrt{w_c}} = \frac{2}{-m\mu B + \sqrt{(m\mu B)^2 + 4m}}$, thus, the transition **A1/A2** occurs at

$$\rho = \frac{2}{-m\mu B + \sqrt{(m\mu B)^2 + 4m}} = \rho_{A1/2}.$$

The case **A2** occurs when $\rho_{A1/2} < \rho < \rho_1(w_\lambda)$, $\lambda > \frac{1}{2 - \alpha}$, or $\rho_{A1/2} < \rho < \rho_T$, $\lambda < \frac{1}{2 - \alpha}$. Comparing with **A1**, in case **A2** one more flat branch, $f_{M2}(w)$, appears in the definition of the map:

$$(A2) \quad f(w) = \begin{cases} f_L(w) = w^\alpha, & \text{if } w < w''', \\ f_{M2}(w) = \left(\frac{\gamma}{\rho}\right)^\gamma, & \text{if } w''' < w < w_\rho, \\ f_{R2}(w) = \left(\frac{\gamma}{\mu B}(1 - w/m_2)\right)^\gamma, & \text{if } w_\rho < w < w_\mu, \\ f_{R3}(w) = \left(\frac{\gamma}{B}\right)^\gamma, & \text{if } w > w_\mu. \end{cases} \quad (12)$$

For (2), we have that $w''' = 1/\rho^2$. An example of map f in case A2 is shown in Fig. 1(b). If $\rho_{A1/2} < \rho < \rho_1(w_\lambda)$, $\lambda < \frac{1}{2 - \alpha}$ and $\rho > \rho_T$ (Case **A2'**), map f is given as

$$(A2') \quad f(w) = \begin{cases} f_L(w) = w^\alpha, & \text{if } w < w', \\ f_{M1}(w) = \left(\frac{\gamma\lambda}{\rho} \frac{1}{(1-w/m_1)} \right)^\gamma, & \text{if } w' < w < w'', \\ f_L(w) = w^\alpha, & \text{if } w'' < w < w''', \\ f_{M2}(w) = \left(\frac{\gamma}{\rho} \right)^\gamma, & \text{if } w''' < w < w_\rho, \\ f_{R2}(w) = \left(\frac{\gamma}{\mu B} (1 - w/m_2) \right)^\gamma, & \text{if } w_\rho < w < w_\mu, \\ f_{R3}(w) = \left(\frac{\gamma}{B} \right)^\gamma, & \text{if } w > w_\mu. \end{cases} \quad (13)$$

An example of map f in case A2' is shown in Fig. 1(c).

The transition **A2/A3** (and **A2'/A3**) occurs when $\rho = \rho_1(w_\lambda)$, that is for $\rho = \rho_{A2/3}$ (see (6)). In the special case (2), we have

$$\rho_{A2/3} = \frac{1}{\sqrt{(1-\lambda)m}} \quad \text{or} \quad \lambda_{A2/3} = 1 - \frac{1}{m\rho^2}. \quad (14)$$

The case **A3** occurs when $\rho > \rho_1(w_\lambda)$, i.e. $\rho > \rho_{A2/3}$. The map f in this case is given as

$$(A3) \quad f(w) = \begin{cases} f_L(w) = w^\alpha, & \text{if } w < w', \\ f_{M1}(w) = \left(\frac{\gamma\lambda}{\rho} \frac{1}{(1-w/m_1)} \right)^\gamma, & \text{if } w' < w < w_\lambda, \\ f_{M2}(w) = \left(\frac{\gamma}{\rho} \right)^\gamma, & \text{if } w_\lambda < w < w_\rho, \\ f_{R2}(w) = \left(\frac{\gamma}{\mu B} (1 - w/m_2) \right)^\gamma, & \text{if } w_\rho < w < w_\mu, \\ f_{R3}(w) = \left(\frac{\gamma}{B} \right)^\gamma, & \text{if } w > w_\mu. \end{cases} \quad (15)$$

An example of map f in case A3 is shown in Fig. 1(f).

Case B: $w_\lambda > w_c$. Let now $w_\lambda > w_c$, i.e., $\lambda < \lambda_{A/B}$ where $\lambda_{A/B}$ is given in (9) (see the region below the line $\lambda_{A/B}$ in Fig. 1(e)). Again, we need to distinguish between several subcases depending on the value of ρ .

The case **B1** occurs when $\rho < \rho_1(\hat{w}) = \rho_2(\hat{w}) =: \rho_{B1/2}$, $\lambda < \lambda^*$ or $\rho < \rho_T$, $\lambda > \lambda^*$, where λ^* is defined in (8) and ρ_T in (5). The corresponding map is given by

$$(B1) \quad f(w) = \begin{cases} f_L(w) = w^\alpha, & \text{if } w < \hat{w}, \\ f_{R1}(w) = \left(\frac{\gamma\lambda}{\mu B} \frac{(1 - w/m_2)}{(1 - w/m_1)} \right)^\gamma, & \text{if } \hat{w} < w < w_\lambda, \\ f_{R2}(w) = \left(\frac{\gamma}{\mu B} (1 - w/m_2) \right)^\gamma, & \text{if } w_\lambda < w < w_\mu, \\ f_{R3}(w) = \left(\frac{\gamma}{B} \right)^\gamma, & \text{if } w > w_\mu. \end{cases} \quad (16)$$

The branch $f_{R1}(w)$ is decreasing if $m_1 > m_2$, increasing if $m_1 < m_2$, and it can be convex or concave. For $m_1 = m_2$ it is flat, $f_{R1}(w) = \frac{\lambda}{\mu B}$. See an example of map f in case B1 in Fig. 1(g). If $\rho < \rho_{B1/2}$, $\lambda > \lambda^*$ and $\rho > \rho_T$, then we have case **B1'** when map f is given by

$$(B1') \quad f(w) = \begin{cases} f_L(w) = w^\alpha, & \text{if } 0 < w < w', \\ f_{M1}(w) = \left(\frac{\gamma\lambda}{\rho} \frac{1}{(1-w/m_1)} \right)^\gamma, & \text{if } w' < w < w'', \\ f_L(w) = w^\alpha, & \text{if } w'' < w < \hat{w}, \\ f_{R1}(w) = \left(\frac{\gamma\lambda}{\mu B} \frac{(1-w/m_2)}{(1-w/m_1)} \right)^\gamma, & \text{if } \hat{w} < w < w_\lambda, \\ f_{R2}(w) = \left(\frac{\gamma}{\mu B} (1-w/m_2) \right)^\gamma, & \text{if } w_\lambda < w < w_\mu, \\ f_{R3}(w) = \left(\frac{\gamma}{B} \right)^\gamma, & \text{if } w > w_\mu. \end{cases} \quad (17)$$

Fig. 1(i) shows example of map f in case B1'.

The case **B2** occurs when $\rho_1(\hat{w}) = \rho_2(\hat{w}) < \rho < \frac{B\mu}{1 - (1-\lambda)m_1/m_2} =: \rho_{B2/3}$ (it holds that $w_\rho \leq w_\lambda$ for $\rho \leq \rho_{B2/3}$), and the map is given by

$$(B2) \quad f(w) = \begin{cases} f_L(w) = w^\alpha, & \text{if } w < w', \\ f_{M1}(w) = \left(\frac{\gamma\lambda}{\rho} \frac{1}{(1-w/m_1)} \right)^\gamma, & \text{if } w' < w < w_\rho, \\ f_{R1}(w) = \left(\frac{\gamma\lambda}{\mu B} \frac{(1-w/m_2)}{(1-w/m_1)} \right)^\gamma, & \text{if } w_\rho < w < w_\lambda, \\ f_{R2}(w) = \left(\frac{\gamma}{\mu B} (1-w/m_2) \right)^\gamma, & \text{if } w_\lambda < w < w_\mu, \\ f_{R3}(w) = \left(\frac{\gamma}{B} \right)^\gamma, & \text{if } w > w_\mu. \end{cases} \quad (18)$$

Here the branch $f_{M1}(w)$ is increasing and convex. An example of map f in case B2 is shown in Fig. 1(j).

The transition **B1/B2** (and **B1'/B2**) occurs when

$$\rho = \rho_1(\hat{w}) = \rho_2(\hat{w}) = \frac{B\mu}{1 - \frac{\hat{w}}{m_2}} =: \rho_{B1/2},$$

where \hat{w} satisfies (7). For the special case (2), $\rho_1(\hat{w}) = \rho_2(\hat{w})$ occurs when

$$\rho = \frac{mB\mu}{m - \left(\frac{\lambda}{B\mu} \right)^2} =: \rho_{B1/2}.$$

The case **B3** occurs when $\rho_1(\hat{w}) = \rho_2(\hat{w}) < \rho$ and $\rho > \rho_{B2/3}$, then the map is given by

$$(B3) \quad f(w) = \begin{cases} f_L(w) = w^\alpha, & \text{if } w < w', \\ f_{M1}(w) = \left(\frac{\gamma\lambda}{\rho} \frac{1}{(1-w/m_1)} \right)^\gamma, & \text{if } w' < w < w_\lambda, \\ f_{M2}(w) = \left(\frac{\gamma}{\rho} \right)^\gamma, & \text{if } w_\lambda < w < w_\rho, \\ f_{R2}(w) = \left(\frac{\gamma}{\mu B} (1-w/m_2) \right)^\gamma, & \text{if } w_\rho < w < w_\mu, \\ f_{R3}(w) = \left(\frac{\gamma}{B} \right)^\gamma, & \text{if } w > w_\mu. \end{cases} \quad (19)$$

The new branch $f_{M2}(w)$ in the definition of f is flat. See an example of map f in case B3 in Fig. 1(k).

The transition **B2/B3** occurs when

$$\rho = \frac{B\mu}{1 - (1 - \lambda) \frac{m_1}{m_2}} = \rho_{B2/3},$$

and, for (2),

$$\rho = \frac{B\mu}{\lambda} = \rho_{B2/3} \quad \text{or} \quad \lambda = \frac{B\mu}{\rho} = \lambda_{B2/3}$$

(see Fig. 1(e)).

On behalf of all authors, the corresponding author states that there is no conflict of interest.

References

1. P. Aghion, A. Banerjee, T. Piketty, *Dualism and macroeconomic volatility*, Q. J. Econ., **114**, 1359–1397 (1999).
2. V. Avrutin, L. Gardini, I. Sushko, F. Tramontana, *Continuous and discontinuous piecewise-smooth one-dimensional maps: invariant sets and bifurcation structures*, World Sci. Ser. Nonlinear Sci. Ser. A, vol. 95, World Sci. (2019); DOI: 10.1142/8285.
3. V. Avrutin, M. Schanz, S. Banerjee, *Multi-parametric bifurcations in a piecewise-linear discontinuous map*, Nonlinearity, **19**, 1875–1906 (2006); DOI:10.1088/0951-7715/19/8/007.
4. S. Banerjee, M. S. Karthik, G. Yuan, J. A. Yorke, *Bifurcations in one-dimensional piecewise smooth maps – theory and applications in switching circuits*, IEEE Trans. Circ. Syst. I, **47**, 389–394 (2000).
5. S. Banerjee, J. A. Yorke, C. Grebogi, *Robust chaos*, Phys. Rev. Lett., **80**, № 14, 3049–3052 (1998).
6. S. Banerjee, G. C. Verghese (Eds.), *Nonlinear phenomena in power electronics: attractors, bifurcations, chaos, and nonlinear control*, IEEE Press, New York (2001).
7. B. Brogliato, *Nonsmooth mechanics – models, dynamics and control*, Springer-Verlag, New York (1999).
8. A. Colombo, F. Dercole, *Discontinuity induced bifurcations of nonhyperbolic cycles in nonsmooth systems*, SIAM J. Imaging Sci., **3**, № 1, 62–83 (2010).
9. W. de Melo, S. van Strien, *One-dimensional dynamics*, Springer-Verlag, New York (1991).
10. M. di Bernardo, C. J. Budd, A. R. Champneys, P. Kowalczyk, *Piecewise-smooth dynamical systems: theory and applications, applied mathematical sciences*, vol. 163, Springer-Verlag, London (2007).
11. L. Gardini, I. Sushko, A. Naimzada, *Growing through chaotic intervals*, J. Econom. Theory, **143**, 541–557 (2008).
12. B. L. Hao, *Elementary symbolic dynamics and chaos in dissipative systems*, World Sci., Singapore (1989).
13. C. Hommes, H. Nusse, *Period three to period two bifurcation for piecewise linear models*, J. Economics, **54**, № 2, 157–169 (1991).

14. W. Huang, R. Day, *Chaotically switching bear and bull markets: the derivation of stock price distributions from behavioral rules*, Nonlinear Dynamics and Evolutionary Economics, Oxford Univ. Press, Oxford (1993), p. 169–182.
15. S. Ito, S. Tanaka, H. Nakada, *On unimodal transformations and chaos II*, Tokyo J. Math., **2**, 241–259 (1979).
16. K. Ichimura, M. Ito, *Dynamics of skew tent maps*, RIMS Kokyuroku, 92–98 (1998).
17. K. L. Judd, *On the performance of patents*, Econometrica, **53**, 567–586 (1985).
18. Y. L. Maistrenko, V. L. Maistrenko, L. O. Chua, *Cycles of chaotic intervals in a time-delayed Chua's circuit*, Int. J. Bifur. Chaos, **3**, 1557–1572 (1993).
19. K. Matsuyama, *Growing through cycles*, Econometrica, **67**, 335–347 (1999).
20. K. Matsuyama, *Credit traps and credit cycles*, Amer. Econom. Rev., **97**, 503–516 (2007).
21. K. Matsuyama, *The good, the bad, the ugly: an inquiry into the causes and nature of credit cycles*, Theor. Econom., **8**, 623–651 (2013).
22. K. Matsuyama, I. Sushko, L. Gardini, *Revisiting the model of credit cycles with good and bad projects*, J. Econom. Theory, **163**, 525–556 (2016); DOI: 10.1016/j.jet.2016.02.010.
23. N. Metropolis, M. L. Stein, P. R. Stein, *On finite limit sets for transformations on the unit interval*, J. Combin. Theory, **15**, 25–44 (1973).
24. M. Misiurewicz, E. Visinescu, *Kneading sequences of skew tent maps*, Ann. Inst. Henri Poincaré Probab. Stat., **27**, 125–140 (1991).
25. H. E. Nusse, J. A. Yorke, *Border-collision bifurcations including period two to period three for piecewise smooth systems*, Physica D, **57**, 39–57 (1992).
26. H. E. Nusse, J. A. Yorke, *Border-collision bifurcation for piecewise smooth one-dimensional maps*, Int. J. Bifur. and Chaos, **5**, 189–207 (1995).
27. A. Sharkovsky, S. Kolyada, A. Sivak, V. Fedorenko, *Dynamics of one-dimensional maps*, Kluwer Acad., Dordrecht (1997).
28. I. Sushko, A. Agliari, L. Gardini, *Bifurcation structure of parameter plane for a family of unimodal piecewise smooth maps: border-collision bifurcation curves*, Chaos, Solitons & Fractals, **29**, Issue 3, 756–770 (2006).
29. I. Sushko, L. Gardini, *Degenerate bifurcations and border collisions in piecewise smooth 1D and 2D maps*, Int. J. Bifur. and Chaos, **20**, 2045–2070 (2010).
30. I. Sushko, L. Gardini, K. Matsuyama, *Superstable credit cycles and U-sequence*, Chaos, Solitons & Fractals, **59**, 13–27 (2014); DOI: 10.1016/j.chaos.2013.11.006.
31. I. Sushko, L. Gardini, K. Matsuyama, *Robust chaos in a credit cycle model defined by a one-dimensional piecewise smooth map*, Chaos, Solitons & Fractals, **91**, 299–309 (2016); DOI: 10.1016/j.chaos.2016.06.015.
32. F. Tramontana, L. Gardini, F. Westerhoff, *Heterogeneous speculators and asset price dynamics: further results from a one-dimensional discontinuous piecewise-linear model*, Comput. Economics, **38**, 329–347 (2011).
33. Z. T. Zhusubaliyev, E. Mosekilde, *Bifurcations and chaos in piecewise-smooth dynamical systems*, World Sci., Singapur (2003).

Received 01.08.23